

1. Artistically Impressive:

NL Rosi, CS Thaxton, CA Mirkin. "Control of Nanoparticle Assembly Using DNA-Modified Diatom Templates". *Angewandte Chemie International Edition*, **43**, Issue 41 (p 5500-5503).

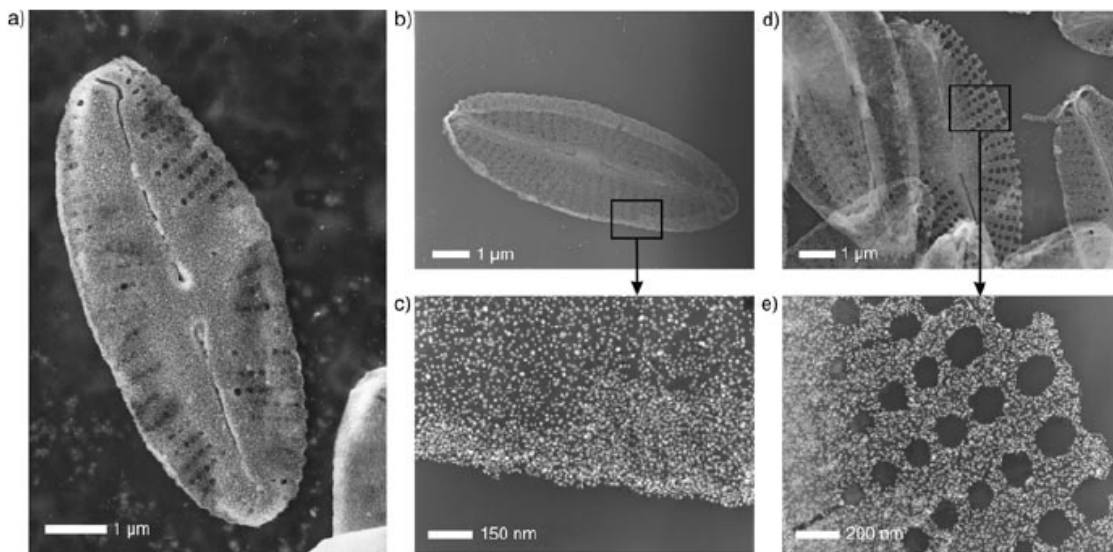


Figure 4. Electron microscope images of DNA-functionalized *Navicula* diatoms densely coated with one layer of DNA-modified 13 nm gold particles. SEM (a) and TEM images (b,c) both reveal a dense outer coating of nanoparticles on the *Navicula* surface. The homogeneous nanoparticle coating of the highly symmetric and nanoscopically detailed *Navicula* template is further illustrated in d) and e), which are different magnifications of a single frustule.

Scientifically Impressive:

MH Huang, *et al*, "Room-Temperature Ultraviolet Nanowire Nanolasers" *Science* **292**, (2001) 1897.

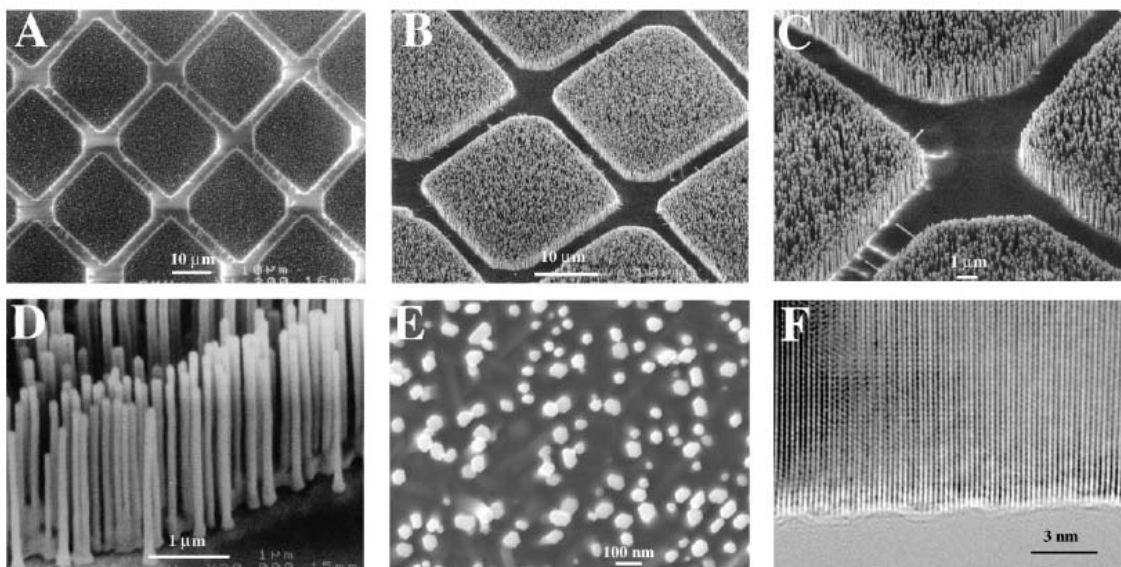


Fig. 1. (A through E) SEM images of ZnO nanowire arrays grown on sapphire substrates. A top view of the well-faceted hexagonal nanowire tips is shown in (E). (F) High-resolution TEM image of an individual ZnO nanowire showing its <0001> growth direction. For the nanowire growth, clean (110) sapphire substrates were coated with a 10 to 35 Å thick layer of Au, with or without using TEM grids as shadow masks (micro contact printing of thiols on Au followed by selective etching has also been used to create the Au pattern).

An equal amount of ZnO powder and graphite powder were ground and transferred to an alumina boat. The Au-coated sapphire substrates were typically placed 0.5 to 2.5 cm from the center of the boat. The starting materials and the substrates were then heated up to 880° to 905°C in an Ar flow. Zn vapor is generated by carbothermal reduction of ZnO and transported to the substrates where ZnO nanowires grow. The growth generally took place within 2 to 10 min (15).

Technically Impressive:

XY Kong, *et al.* "Single-Crystal Nanorings Formed by Epitaxial Self-Coiling of Polar Nanobelts. *Science* **303**, (2004) 1348.

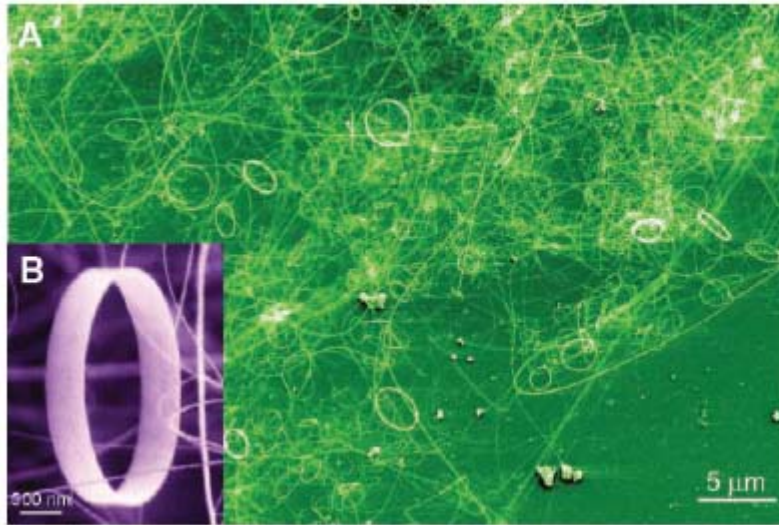


Fig. 1. (A) Low-magnification SEM image of the as-synthesized ZnO nanorings. (B) High-magnification SEM image of a freestanding single-crystal ZnO nanoring, showing uniform and perfect geometrical shape. The ring diameter is 1 to 4 μm , the thickness of the ring is 10 to 30 nm, and the width of the ring shell is 0.2 to 1 μm .

2. Backscattered Electron Analysis – The production of backscattered electrons is strongly dependant on the average atomic number of the sample. Backscattered electrons can be useful in determining the presence of differences in average atomic number of a sample.

Auger Electron Analysis – Measurement of the energy level of Auger electrons may be useful in determining the composition of the top 1 nm of a sample. It is most useful in the range of atomic numbers from 2 to 10, which is especially useful since low Z materials are difficult to analyze using backscattered electron or x-ray analysis.

Cathodoluminescence – The production of light by conductors, semiconductors and insulators is a result of electron transistions actoss forbidden band gaps or quantum well band structures. It is especially useful in mineralogy and chemistry, and has limited biological applications, such as the detection of calcified regions of aortas and herbicide detection.

Electron-Channeling Contrast – An electron beam entering a sample will produce more backscattered electrons if the beam enters perpendicular to lattice planes, and fewer if it enters parallel to the planes of the lattice structure, since it will penetrate the sample deeper, and fewer of the electrons will be able to escape due to absorption. This produces a difference in contrast. It is only useful in imaging large samples (10 mm square) at very low magnification, because the technique relies on wide angle deviation of the electron beam. The technique is useful for showing crystallographic features such as grains and twists, since the grains have the planes located in different directions, and each produces electron-channeling contrast.

Selected-Area Electron-Channeling – A much more useful form of electron-channeling contrast that rocks the electron beam back and forth through a cone of incident angles at high magnifications. This allows electron-channeling contrast analysis to be performed on much smaller areas. This technique has a special resolution of 1 μm and an angular resolution of 1° to 2° , and requires a carefully polished sample.

Electron-Backscattered Patterns – A stationary electron beam strikes a sample tilted on an angle, and a nearby electron negative or electron recording device placed parallel to the

beam records the backscattered electrons as they are diffracted outward after striking the crystallographic planes. This technique has a special resolution of 20 nm and an angular resolution of 1° to 2°, and requires a carefully polished sample.

Micro-Kossel X-ray Diffraction Patterns – A stationary electron beam strikes a sample tilted on an angle, and a nearby window transparent to x-rays, such as a beryllium thin-film, which prevents the passage of electrons, is placed parallel to the beam. The x-rays strike the film after they are diffracted outward due to striking the crystallographic planes. This is similar to Electron-Backscattered Patterns, except that x-rays are used in the generation of these patterns. This technique has a special resolution of 100 nm and an angular resolution of 0.01°, and can be used with a rough sample.

Sample Current or Absorbed Current Imaging – This technique relies on variation in current flow during scanning, and is relatively independent of surface topology. This technique is mainly used to allow internal variations to be visualized. A sample-current image is typically inverted contrast of the backscattered electron image.

Voltage-Contrast Imaging – Small voltages placed on small areas of a sample can create variations in brightness of the sample, for example positive voltages may cause fewer secondary electrons to escape, making that area appear darker. Voltage-contrast imaging is particularly important in the development of semiconductors and integrated circuits, since it is possible to observe the various circuit pathways while the device is in operation, since areas of high current flow appear brighter.

Magnetic Contrast – Magnetic fields above the sample deflect the secondary electrons, producing changes in contrast. This type of magnetic imaging has been used to observe the magnetic domains on recording tape. Internal magnetic fields can also affect the scattering of electrons. Backscattered electrons can be used in this case to show differences in the magnetic domains. Magnetic contrast imaging of both types is useful in the study of magnetic memory devices.

Electron-Beam Induced Current – When an electron beam is focused on a p-n junction, the incident electrons can generate electron-hole pairs that produce a current in the device. The current contrast can be used to produce an image. Electron-Beam induced current is mainly used for semiconductor analysis.

Energy Dispersive X-Ray Spectroscopy (EDS) – EDS measures the energy of x-rays produced by the sample in order to determine the elements present by analysis of the characteristic x-rays produced by each element. EDS can be used to produce a listing of the elements present, a plot of the x-ray spectrum, and a mapping of a sample showing the locations of various elements.

Wavelength Dispersive X-Ray Spectroscopy (WDS) – WDS measures the wavelengths of x-rays produced in a sample. A WDS system may cost four times as much as an EDS system, and it is usually possible to detect no more than four elements at a time. Each detector must be adjusted to the correct wavelength for each element separately, and most systems have no more than four detectors. The most important advantage of WDS over EDS is that it has a spectral selectivity of 10 eV, as compared to 135 eV in EDS.

However, due to advanced signal processing techniques such as peak deconvolution, this advantage is minimal when compared to the advantages of EDS. (SL Flegler, JW Heckman and KL Klomparens, *Scanning and Transmission Electron Microscopy: An Introduction*. Oxford University Press (1993). ISBN 0-19-510751-9)

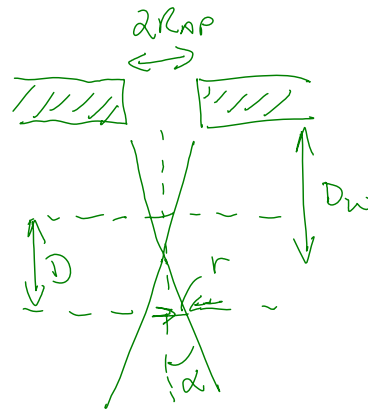
3. "Most SEMs have a working distance that varies from about 10 mm to 40 mm or 50 mm. A large working distance results in a narrow cone of electrons, a small one in a wide cone." (SL Flegler, JW Heckman and KL Klomparens, *Scanning and Transmission Electron Microscopy: An Introduction*. Oxford University Press (1993). ISBN 0-19-510751-9) The SEM in the basement of the plant sciences building has a working distance that ranges from 8 mm to 39 mm. 8 mm is used for the highest resolution, especially at high magnification; 39 mm is used for the highest depth of field, especially at low magnification. The smallest aperture is typically around 100 μm in diameter, so this is the value I will use in deriving the depth of field. This calculation is attached to the end of this homework submission. The working distances in between are used to optimize depth of field and image quality for many different types of samples.

Monday, February 04, 2008
1:49 PM

$$\tan \alpha = \frac{R_{AP}}{D_w} = \frac{r}{\frac{1}{2}D}$$

$$\therefore D = \frac{2r D_w}{R_{AP}}$$

$$r \approx \frac{100 \mu\text{m}}{\text{MAG}} \Rightarrow D = \frac{200 \mu\text{m} D_w}{\text{MAG} \times R_{AP}}$$



$$D \approx \frac{200 \mu\text{m} \times 50 \text{ mm}}{20,000 \times 50 \mu\text{m}} \frac{10^3 \mu\text{m}}{1 \text{ mm}} \approx 10 \mu\text{m}, \text{ PRETTY GOOD}$$

4. X-rays are capable of producing additional x-rays when they strike any material in a similar manner to the way that the electron beam produces x-rays. X-rays produced in the sample can fluoresce nearby materials, and these fluoresced x-rays, which are characteristic of the nearby materials and not the sample, can be detected to give false data about the sample's composition. Materials that are directly above the sample and materials in between the sample and x-ray detector are particularly problematic for x-ray fluorescence errors. (SL Flegler, JW Heckman and KL Klomparens, *Scanning and Transmission Electron Microscopy: An Introduction*. Oxford University Press (1993). ISBN 0-19-510751-9)